Molecular Neurobiology (2019) 56:8109–8123
https://doi.org/10.1007/s12035-019-01656-z

Neuroprotective Effects of AG490 in Neonatal Hypoxic-Ischemic Brain Injury

Feiya Li[1,2] · Raymond Wong[1,2] · Zhengwei Luo[1,2] · Lida Du[1,2] · Ekaterina Turlova[1,2] · Luiz R. G. Britto[3] · Zhong-Ping Feng[2] · Hong-Shuo Sun[1,2,4,5]

Received: 31 January 2019 / Accepted: 20 May 2019 / Published online: 12 June 2019

Abstract

In infants and children, neonatal hypoxic-ischemic (HI) brain injury represents a major cause of chronic neurological morbidity. The transient receptor potential melastatin 2 (TRPM2), a non-selective cation channel that conducts calcium, can mediate neuronal death following HI brain injury. An important endogenous activator of TRPM2 is H_2O_2, which has previously been reported to be upregulated in the neonatal brain after hypoxic ischemic injury. Here, incorporating both in vitro (H_2O_2-induced neuronal cell death model) and in vivo (mouse HI brain injury model) approaches, we examined the effects of AG490, which can inhibit the H_2O_2-induced TRPM2 channel. We found that AG490 elicited neuroprotective effects. We confirmed that AG490 reduced H_2O_2-induced TRPM2 currents. Specifically, application of AG490 to neurons ameliorated H_2O_2-induced cell injury in vitro. In addition, AG490 administration reduced brain damage and improved neurobehavioral performance following HI brain injury in vivo. The neuroprotective benefits of AG490 suggest that pharmacological inhibition of H_2O_2-activated TRPM2 currents can be exploited as a potential therapeutic strategy to treat HI-induced neurological complications.

Keywords Transient receptor potential melastatin 2 · Ion channel · Hypoxic-ischemic brain injury · Neuroprotection · Inhibitor · AG490

Introduction

Neonatal hypoxic-ischemic (HI) brain injury occurs as a result of inadequate levels of oxygen and blood in the neonate's brain [1]. The intensity and length of this deprivation determines the severity of HI brain injury, which manifests as a range of symptoms including transient behavioral abnormalities, occasional periods of apnea, seizures, cardiorespiratory failure, and death [1, 2]. Fifty to eighty percent of survivors suffer from severe developmental delays, motor impairments, and learning disabilities [2, 3]. The lifetime cost is estimated to be ~$1.5 million per person in Canada [2]; thus, HI brain injury represents a serious socioeconomic burden on the healthcare systems. Currently, the standard treatment for neonatal HI brain injury is hypothermia [4–6]. Although previous clinical studies evaluating hypothermia (33–34 °C) showed a reduction in disability and mortality, the conclusion was that hypothermia as a treatment for HI brain injury is only partially effective [7, 8]. Therefore, there is an urgent need for a more effective and potent treatment.

The exact pathophysiology of HI brain injury remains ill-defined. Insufficient blood flow combined with decreased blood oxygen results in abnormal cerebral autoregulation and brain injury [9, 10]. Because the reduction in blood flow can lead to excessive glutamate release (which can cause excitotoxicity and ultimately HI brain injury) [11], glutamate receptors, as potential therapeutic targets, have traditionally

Feiya Li, Raymond Wong and Zhengwei Luo contributed equally to this work.

✉ Zhong-Ping Feng
zp.feng@utoronto.ca

✉ Hong-Shuo Sun
hss.sun@utoronto.ca

[1] Department of Surgery, Faculty of Medicine, University of Toronto, 1 King's College Circle, Toronto, Ontario M5S 1A8, Canada

[2] Department of Physiology, Faculty of Medicine, University of Toronto, 1 King's College Circle, Toronto, Ontario M5S 1A8, Canada

[3] Department of Physiology and Biophysics, Institute of Biomedical Sciences, University of São Paulo, São Paulo, Brazil

[4] Department of Pharmacology and Toxicology, Faculty of Medicine, University of Toronto, Toronto, Ontario M5S 1A8, Canada

[5] Institute of Medical Science, Faculty of Medicine, University of Toronto, Toronto, Ontario M5S 1A8, Canada

been the main research focus. However, clinical trials evaluating several NMDA inhibitors did not yield therapeutic benefits in human patients even though they showed promising neuroprotective effects in rodent models [9, 10, 12]. This suggests that non-glutamate mechanisms may also play important roles in mediating brain damage induced by ischemia and/or hypoxia. Therefore, it is critical to elucidate non-glutamate mechanisms and establish appropriate novel drug targets and corresponding drugs.

The transient receptor potential melastatin 2 (TRPM2) belongs to the TRP superfamily of ion channels. TRPM2 is expressed in the brain (including neurons, microglia) and has been implicated in mediating neurotoxicity [13–15]. It has been speculated that since TRPM2 conducts Ca^{2+}, excessive TRPM2 activity can lead to cytotoxicity due to Ca^{2+} overload [13]. There is evidence showing that TRPM2 is involved in several CNS pathologies, including stroke, Alzheimer's disease, and bipolar disorder [16–18]. TRPM2 can be activated by H_2O_2, which has previously been reported to be upregulated following HI brain injury [14, 15, 19]. And so, it is speculated that there is excessive TRPM2 activity following HI insult. Recently, in vivo studies from us and others have shown that knockout of TRPM2 in rodent models conferred neuroprotective effects following ischemic and hypoxic brain injuries [20, 21]. Specifically, TRPM2 knockout reduced ischemic brain damage in the adult mouse middle cerebral artery occlusion model [20]. In neonatal mice, we recently demonstrated that TRPM2 knockout also provided neuroprotection following HI brain injury [21]. Therefore, there is strong evidence that TRPM2 is a promising drug target for the treatment of HI brain injury. However, there is currently no in vivo study examining the neuroprotective effects of pharmacological inhibition of TRPM2.

Although the discovery of TRPM2 antagonists has been elusive, AG490 was identified to have an inhibitory effect on TRPM2 [22]. A recent study reported that AG490 potently inhibited H_2O_2-induced intracellular Ca^{2+} influx and significantly reduced H_2O_2-induced TRPM2 currents [22]. Note that, whereas H_2O_2 can also activate the TRPA1 channel, AG490 elicits no effect on TRPA1 current [22]. This suggests the relative specificity of AG490 for H_2O_2-induced TRPM2 currents. Because AG490 was also used as a JAK2 inhibitor, Shimizu et al. [22] examined whether the inhibitory effect of AG490 on TRPM2 was due to JAK2 inhibition by testing the effects of other JAK2 inhibitors. The study reported that none of the other JAK2 inhibitors had an effect on TRPM2 currents, thus suggesting that the inhibitory effects of AG490 on TRPM2 is independent of JAK2 inhibition [22]. The study also examined the effects of JAK2 inhibitors (pyridine 6 or staurosporine) on TRPM2 currents but none of them showed inhibitory effects [22].

In the present study, we evaluated AG490 in neonatal HI brain injury. We confirmed that AG490 reduced H_2O_2-activated TRPM2 currents. Specifically, we demonstrate that AG490 confers neuroprotection by showing its in vitro effects on H_2O_2-induced neuronal cell death and in vivo effects on neonatal HI brain injury. Because there is currently no pharmacological manner of prevention and treatment for HI brain injury, our findings here can contribute to potential drug development.

Materials and Methods

Animals/Ethics

P7 pups (with P0 defined as the day of birth) were used in this study. Pups were obtained from timed-pregnant CD-1 mice, which were purchased from Charles River Laboratories (Sherbrooke, QB, Canada). Animals were housed at 20 ± 1 °C in a 12-h light/dark cycle. Food (standard laboratory chow diet) and water were readily accessible. All protocols were carried out strictly according to the Canadian Council on Animal Care (CCAC protocol) guidelines.

Cell Culture

TRPM2-overexpressed HEK293 cells were cultured as follows: doxycycline-inducible HEK293 cells stably expressing TRPM2 were cultured with DMEM containing: 10% FBS, 1% antibiotic-antimycotic, blasticidin (5 μg/ml, Sigma-Aldrich, USA), and zeocin (0.4 mg/ml, Invitrogen, USA). TRPM2 expression was induced with doxycycline (1 μg/ml, Sigma-Aldrich, USA) for > 24 h.

Primary neurons were cultured from E16 CD-1 mice. Dissected cortices were digested with 0.025% trypsin/EDTA at 37 °C for 15 min. Cell density was with an Improved Neubauer hemocytometer, and 1.0 × 104 cells were plated on poly-D-lysine-coated glass coverslips (12 mm no. 1 German Glass, Bellco cat. no. 1943-10012, Sigma-Aldrich, USA). The cells were maintained in culture medium (neurobasal medium supplemented with 1.8% B27, 0.25% Glutamax, and 1% antibiotic-antimycotic) at 5% CO_2 and 37 °C.

Drug Administration

In Vitro Administration Various concentrations of AG490 were prepared by dissolving in B27-free culture medium. As a pre-treatment, AG490 was added to the culture media of cells prior to exposing cells to H_2O_2.

In Vivo Administration Pups weighting ~ 5 g were randomly assigned into: sham control group (Sham), HI + vehicle (vehicle; 5% DMSO and 5% Tween 80 in 0.9% saline) or HI + AG490 (AG490; 30 mg/kg). AG490 was dissolved in 5%

DMSO and 5% Tween 80 (P-8074) in 0.9% saline for the final concentration of 30 mg/kg. AG490 (30 mg/kg) or vehicle control was administered to the pups either: (1) 20 min prior to ischemic induction (pre-treatment); (2) following ischemic induction (post-treatment 1); or (3) immediately after both ischemia and hypoxia (post-treatment 2). The compound was administered intraperitoneally (i.p.) at 20 μl/g (injection ratio to body weight).

In Vitro Cell Death Model/Cell Viability Assays

The H_2O_2-induced cell death in vitro model was carried out using CD-1 E16 embryos. Thirty percent stock H_2O_2 solution was diluted (by 100-fold) into culture medium prior to each experiment. This was then added to the cells in a 96-well plate. After exposure to H_2O_2, the plate was kept at 5% CO_2 and 37 °C for 24 h before toxicity or biochemical assessments were conducted.

The MTT assay was carried out as previously described [23, 24]. In brief, because MTT (yellow) is reduced by oxidoreductase enzymes in viable cells to produce an insoluble formazan (purple), the ratio of yellow MTT to purple formazan indicates the number of viable cells. Cells were seeded at a density of 5×10^4 cells/ml, and subsequently treated with various concentrations of AG490 for 24 h. MTT (0.5 mg/ml MTT in PBS) was diluted with culture medium with a dilution ratio of 1:10 and added to each well. After incubation (3 h), the medium was removed from each well and 100 μl DMSO was added. The absorbance at 490 nm was measured in a microplate reader (Syngery H1, Biotek, USA), and viability was expressed as a percentage of the control.

Cell death assessment was performed by staining cells with propidium iodide (PI), which is a fluorescent intercalating agent [25]. Since PI cannot permeate live cells, it can differentiate between necrotic and healthy cells. Twenty-four hours following the addition of AG490, cells were stained with PI (1 μg/ml), and the fluorescent intensity was measured by a Synergy HT Multi-Mode Micro plate reader.

Electrophysiology

Patch clamp recordings in the whole cell configuration were carried out at room temperature using an Axopatch 700B (Axon Instruments, Inc.) to examine the effects of AG490 on TRPM2 currents in TRPM2-overexpressed HEK293 cells or primary cortical neurons from E16 CD-1 mice [22, 26]. TRPM2-overexpressed HEK293 cells were induced with 1 μg/ml doxycycline at least 24 h before whole cell patch clamping. Currents were recorded using a 400-ms voltage ramp protocol (− 100 to + 100 mV) with an interval of 5 s at 2 kHz and digitized at 5 kHz. Clampex 9.2 was used for data generation, and Clampfit 9.2 was used for data analysis (pClamp). Patch pipette resistance was between 5 and 9 MΩ after filling with pipette solution, which contains (in mM): 145 cesium methanesulfonate, 8 NaCl, 10 EGTA, and 10 HEPES with pH adjusted to 7.2 with CsOH. The bath solution contained (in mM): 140 NaCl, 5 KCl, 2 $CaCl_2$, 20 HEPES, and 10 glucose with pH adjusted to 7.4 with NaOH.

In Vivo Hypoxic-Ischemic Mouse Model

Mouse HI model was performed as previously described with modifications [27–29]. In brief, postnatal day 7 (P7) mice were anesthetized with isoflurane (3.0% for induction and 1.5% for maintenance). The process contained two main goals: ischemia and hypoxia. To induce ischemia, the right common carotid artery was isolated and then ligated with a bipolar electrocoagulation device (Vetroson V-10 Bi-polar electrosurgical unit, Summit Hill Laboratories, Tinton Falls, NJ, USA). The remaining ligated artery was cut using microscissors. Pups were then returned to their dam and allowed to recover for 1.5 h. After recovery, hypoxia was achieved by placing the pups in a 37 °C chamber (A-Chamber A-15274 with ProOx 110 Oxygen Controller/E-720 Sensor, Biospherix, NY, USA) and perfused with a gas mixture of 7.5% oxygen and 92.5% nitrogen for 60 min. A homoeothermic blanket control unit (K-017484 Harvard Apparatus, Massachusetts, USA) was used to monitor the in-chamber temperature. Animals in sham groups only underwent surgery to expose the artery under anesthesia.

Infarct Volume Measurement, Whole Brain Imaging, and Histological Assessments

TTC Staining/Infarct Volume Measurement 24 h after HI, brains were extracted and coronally sectioned into four ~ 1 mm slices, which were then stained with 1.5% 2,3,5-triphenyltetrazolium chloride (TTC; a redox indicator that can differentiate between metabolically active and inactive tissues) for 20 min at 37 °C to visualize the infarct area. The image analysis software ImageJ (NIH, USA) was used to quantify the infarct area. After correcting for edema, the infarct volumes were calculated according to the following formula: Corrected infarct volume (%) = (contralateral hemisphere volume − (ipsilateral hemisphere volume − infarct volume)) / contralateral hemisphere volume × 100% [21, 28, 30].

Whole Brain Imaging/Nissl Staining Seven days after HI, brains were extracted and imaged to examine the morphological differences between the groups. At this time point, the infarct areas in the brains have undergone liquefactive necrosis. To quantify the severity of histological damage, the brains were sliced into ~ 100 μm coronal sections and stained with 1% Cresyl violet (Nissl). The infarct area was traced using ImageJ. Infarct volume was determined with the following:

infarct volume (%) = infarct volume / contralateral hemisphere volume × 100% [21, 28, 30].

Neurobehavioral Assessments

Short-term neurobehavioral tests (i.e., geotaxic reflex, cliff aversion reflex, grip test) were carried out to assess recovery on 1, 3, and 7 days after HI. These well-documented reflex tests were chosen because they represent the earliest stages of development in mice ([23, 24, 29, 31]), and thus good indicators of sensorimotor function. Specifically, (1) geotaxis reflex examines vestibular and proprioceptive functions [32]; (2) cliff aversion reflex tests the maladaptive impulse behavior [32]; and (3) grip test assesses force and fatigability [32]. In addition, a long-term neurobehavioral test was conducted. The passive avoidance test was used to assess contextual fear learning and memory deficits [33, 34]. Because these abilities are not well developed until later in life, the passive avoidance test was conducted on week 4 post-surgery, which indicated long-term neurobehavioral recovery.

Geotaxis reflex is an automatic, stimulus-bound orientation movement. Pups were laid with head facing down on a 45° inclined plane. The time for the pup to rotate 180° was recorded. For the cliff avoidance test, pups were laid on the edge of a platform, and the time to turn away from the cliff by removing both paws from the edge was recorded. For the grip test, pups were suspended over a cotton pad. Their forepaws were placed on a wire, and the time before the pup let go was recorded.

The passive avoidance test is a 3-day 1-trailed long-term behavioral test that assesses both motor functional recovery, as well as learning and memory recoveries. Three weeks after HI injury, mice in all three groups (sham, HI + vehicle, HI + AG490) underwent the passive avoidance test. The protocol consists of habituation (Day 1), acquisition/conditioning (Day 2), and testing (Day 3). The apparatus consists of two parts separated by a guillotine gate: a large (250 × 250 × 240 mm) illuminated compartment, and a small (195 × 108 × 120 mm) dark compartment with electrical grids on the floor (LE872, Panlab, Harvard Apparatus, Barcelona, Spain). During the habituation session (Day 1), a single mouse was placed into the illuminated compartment and given 1 min to explore. The door to the dark compartment was then opened, and the time for the mouse to enter the dark room was recorded (NB. Mice have innate preference for the dark). During the acquisition/conditioning session (Day 2), the mouse was given 30 s to explore the illuminated compartment, and then allowed to enter the dark compartment. After entering the dark compartment for 3 s, the mouse received an unavoidable foot shock (for 2 s at 0.4 mA). During the testing session (Day 3), after the mouse was placed in the illuminated compartment, the door to the dark compartment was opened after 5 s. The time to enter the dark compartment was recorded (maximal latency was limited at 300 s). Longer latency to enter the dark compartment indicated improved memory performance.

Immunohistochemistry and Confocal Imaging

Brain tissues were collected 7 days after HI and fixed overnight in 4% paraformaldehyde/30% sucrose solution at 4 °C. Brains were sectioned coronally into ~ 50 μm slices using a vibratome (Tissue Sectioning System Microtome Vibratome, HuiYou, China), which were then immunohistochemically stained [21, 28]. Specifically, slices were probed with mouse anti-neuronal nuclei (NeuN) antibody (MAB377, 1:500; Chemicon, Temecula, USA) and anti-glial fibrillary acidic protein (GFAP; ab7260, 1:1000; Abcam, Cambridge, USA) antibody overnight at 4 °C. Next, the sections were incubated with secondary antibodies Alexa 488 and 568 (no. 835724, no. 632115, 1:200; Cell Signaling Technology) for 1 h at room temperature, and then mounted on glass coverslips with ProLong Gold antifade reagent (P36930; Thermo Fisher Scientific, Burlington, CA). Confocal laser microscope (LSM700 Zeiss; Oberkochen, Germany) was used to image the immunostained brain slices. Three brains per treatment group were collected; and three to five coronal slices per brain were imaged at × 40 magnification. At least five randomly selected fields were imaged, and the number of cells was quantified using ImageJ.

Western Blot

The quantification of protein levels with Western blot was conducted as previously described with modifications [21, 28]. In brief, 24 h after HI, mouse brains (ipsilateral and contralateral hemispheres) were collected and frozen on dry ice. Protein extraction was by homogenizing the brain samples in RIPA buffer (that contains a cocktail of proteinase and phosphatase inhibitors), and then incubating at 4 °C for 1 h followed with spin-down (15 min at 13,000 rpm centrifuge). Concentration of protein was determined with the Bio-Rad Protein Assay reagent (Bio-Rad, Hercules, CA). Protein samples (30 μg) were separated with 10% SDS-PAGE gel, and then transferred to a nitrocellulose membrane (350 mA, 90 min). Blocking was done with 5% non-fat milk in Tris-buffered saline (TBS). Blots were incubated at 4 °C overnight with primary antibodies, which included anti-phospho-Akt (no. 9271S, Ser473, 1:1000), anti-Akt (no. 9272S, 1:1000), and anti-GAPDH (no. 2118S, 1:10,000). This was followed with secondary antibody incubation at room temperature. Protein signals were detected with chemiluminescent reagents (PerkinElmer, Mass, USA) and analyzed via exposure to film (HyBlot CL, NJ, USA).

Reagents

AG490 was purchased from TOCRIS (CAS no. 82749-70-0). Thirty percent hydrogen peroxide was from Biobasic (HC4060-500ML). Cresyl violet, TTC (T8877), and DMSO (D2650) were purchased from Sigma-Aldrich (St. Louis, MO, USA). All other reagents (unless specified) were from Sigma-Aldrich.

Statistics and Data Analysis

Data were presented as mean with SEM. Student's *t* test was performed to assess the difference between two groups (i.e., vehicle-treated group versus AG490-treated group). In multiple comparisons, one-way ANOVA followed with the Bonferroni test were used. Significance was defined as $p < 0.05$.

Results

AG490 Protects Neurons from H_2O_2-Induced Cell Injury In Vitro

AG490 Blocks the TRPM2 Currents A recent report demonstrated that AG490 significantly reduced H_2O_2-induced TRPM2 activation [22]. To verify the inhibitory effect of AG490 on TRPM2 currents, we recorded from TRPM2-overexpressed HEK293 cells using the whole-cell patch clamp technique. Doxycycline (1 μg/ml; > 24 h) induced TRPM2 overexpression in the HEK293 cells. As shown in Fig. 1a, perfusion of H_2O_2 (200 μM) elicited a large and outwardly rectifying current of 1497.97 ± 452.03 pA ($n = 3$), whereas pretreatment of cells with AG490 (2 h at 37 °C) reduced the current to 67.33 ± 31.63 pA ($n = 3$; $p = 0.034$). Without induction of HEK293 cells with doxycycline, TRPM2 current was not present and perfusion of H_2O_2 had no effect (data not shown). Additionally, we assessed the effects of AG490 on primary cortical neurons (Fig. 1b). Here, we also observed a robust activation of TRPM2-like current following perfusion of H_2O_2 (79.53 ± 5.49 pA/pF; note that the amplitude and I-V curve are consistent with what is reported in the literature [22, 35]), and pretreatment with AG490 abolished the current (4.87 ± 0.81 pA/pF; $n = 5$/group; $p < 0.01$). Note that all analyses and interpretations were conducted on the H_2O_2-sensitive component of the observed currents, and compared between with or without AG490 treatment (*since we did not use any other inhibitors in our recordings, we cannot rule out the potential contamination of other currents in the shown traces*). Our results verify that AG490 can abolish H_2O_2-induced activation of TRPM2 currents.

We investigated the effects of AG490 on the viability and proliferation of cortical neurons, which are vulnerable to free radicals such as H_2O_2. To test whether AG490 can protect neurons from H_2O_2-induced cell death in vitro, MTT assays were performed to assess cell viability, and PI staining was conducted to assess cell death. As shown in Fig. 2a, hydrogen peroxide produced elicited neuronal death in a dose-dependent manner from 6 to 100 μM ($p < 0.05$, $n = 12$). With AG490 pre-treatment (40 min prior to exposure to H_2O_2), there was improved neuronal survival at the optimum concentration of 50 μM. Consistent with our MTT results, fluorescence of PI staining intensity in neurons was significantly greater following exposure to H_2O_2 in a dose-dependent manner from 6 to 50 μM (Fig. 2b, $p < 0.05$, $n = 9$), which was reduced with AG490 pre-treatment (50 μM; 40 min; $p < 0.05$, $n = 6$). Note that the AG490 concentration used in this current study is based on the original finding by Shimizu et al. [22]. Our in vitro results provide evidence suggesting that AG490 can protect cortical neurons from damage caused by H_2O_2 exposure.

Pre-treatment of AG490 Confers Neuroprotective Effects Against HI Brain Injury In Vivo

In order to optimize the relevant specific time points for the current study, we extracted in situ hybridization data from the *Allen Brain Atlas*. Due to the unavailability of mouse data pertaining to TRPM2 expression levels, we used human brain TRPM2 data [36] and calculated the corresponding mouse developmental age as previously described [37]. The extracted data showed that TRPM2 mRNA expression is high in the cortex and hippocampus [21]. Moreover, TRPM2 expression for human is high at 37 weeks after conception, which corresponds to postnatal 7-day old (P7) mouse. Therefore, we used P7 CD-1 mouse pups for all in vivo experiments. AG490 (30 mg/kg) or vehicle was administered as a single i.p. injection to P7 pups.

AG490 Reduced the Brain Infarct Volume of HI Brain Injury TTC staining was carried out on coronal sections of mouse brains 24 h after HI (representative images of TTC staining are shown in Fig. 3). TTC is a redox indicator and it stains for metabolically active tissues (in red). The white area represents the infarct area and illustrates the metabolically inactive damaged tissue. First, we found that a low dose of AG490 (15 mg/kg, i.p., 20 min before HI) did not offer neuroprotection (Fig. 3a). At 15 mg/kg AG490, the infarct volume was 53.40 ± 9.03% ($n = 11$), which was not significant to that of the vehicle-treated HI group at 50.79 ± 6.53% ($n = 8$). This dosage was determined from the literature [38–41]. However, AG490 pre-treatment with a higher dose (30 mg/kg, i.p., 20 min before HI) significantly reduced brain infarct volume in comparison with the vehicle-treated HI group (Fig. 3b). Infarct volume in the vehicle-treated HI group (vehicle) was 58.00 ± 5.11% ($n = 13$), whereas 30 mg/kg AG490 pre-

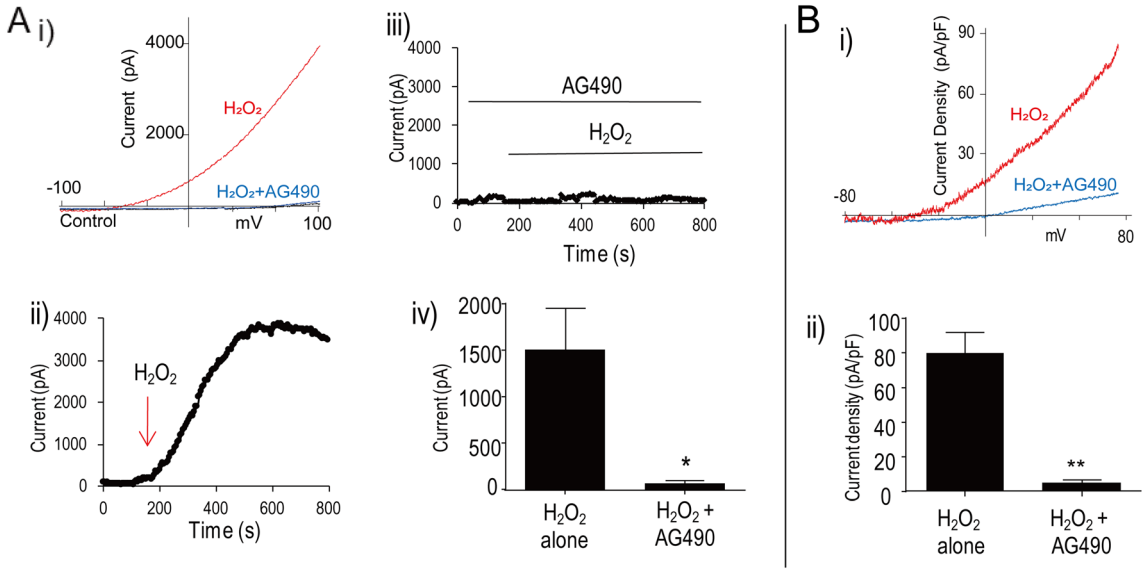

Fig. 1 AG490 inhibited TRPM2 current in HEK293 cells stably overexpressing TRPM2 and primary mouse cortical neurons. **a** i, Representative I-V trace of HEK293 cells induced with doxycycline (black is bath solution; red is perfusion with 200 μM H_2O_2; blue is pre-treatment with 50 μM AG490 for 2 h and perfusion with 200 μM H_2O_2). ii, Time course of H_2O_2-activiated TRPM2 currents in doxycycline-induced TRPM2-overexpressed HEK293 cells. iii, Time course of when doxycycline-induced TRPM2-overexpressed cells were pre-treated with AG490. Note that H_2O_2 failed to activate TRPM2 current. iv, Summary bar chart comparing the H_2O_2-activated TRPM2 currents at + 90 mV with or without application of AG490 (*$p < 0.05$, $n = 3$/group) in HEK293 cells. **b** i, Representative trace of primary mouse cortical neurons (red is H_2O_2 alone; blue is H_2O_2 with AG490 pre-treatment). ii, Summary chart comparing TRPM2 currents with or without AG490 (**$p < 0.01$, $n = 5$/group) in primary cortical neurons

treatment significantly reduced the infarct volume to 22.76 ± 3.11% ($n = 17$; $p < 0.05$). There was no detectable infarction in the sham group (data not shown).

Next, we examined whether the neuroprotective effects of AG490 remained effective 7 days after HI brain injury. Whole brains were collected, fixed, imaged, and then sectioned for Nissl staining. At this time point, the brain infarction had already undergone liquefactive necrosis resulting in loss of brain weight (Fig. 3c). Whole brain weight was used as an indicator of the liquefaction level. There was no detectable brain damage in sham group. The sham and AG490-treated HI groups had greater brain weights in comparison with the vehicle-treated HI group (sham, 0.43 ± 0.01 g; vehicle-treated + HI, 0.33 ± 0.01 g; AG490-treated + HI, 0.37 ± 0.01 g; $p < 0.05$). Whole brains were coronally sliced into ~ 100 μm sections for Nissl staining to reveal that, even 7 days post-HI, animals treated with AG490 sustained less brain damage compared with animals treated with vehicle. In summary, the AG490 (30 mg/kg) pre-treatment group ($n = 15$ pups) demonstrated significantly less brain damage compared with vehicle-treated HI control ($n = 21$ pups). Our findings suggest that AG490 can confer lasting neuroprotection against HI brain injury.

Pre-treatment with AG490 Promotes Recovery After HI Insult Because body weight is one of the most frequently used indicators of general health ([23, 24]), we assessed this parameter of all pups used in the study. Pups were randomly assigned to experimental groups with no significant initial difference in body weights between groups (sham, 5.05 ± 0.08 g; vehicle-treated + HI, 5.08 ± 0.06 g; AG490-treated + HI, 4.93 ± 0.09 g). Weighing was done at four time points: prior to the onset of HI, as well as 1, 3, and 7 days after HI (Fig. 4a). On Day 1 after HI, the mean body weight of the pups that underwent HI surgery was significantly lower compared with the sham group. Seven days after HI, mice in the sham (9.98 ± 0.49 g) and AG490-treated HI groups (9.81 ± 0.50 g) gained significantly more weight than vehicle-treated HI mice (8.32 ± 0.37 g, $p < 0.05$). These results suggested that AG490 pre-treatment promoted general health recovery after exposure to an HI insult.

Short- and Long-Term Neurobehavioral Performances Are Improved After HI with AG490 Pre-treatment To further examine the neuroprotective effects of AG490, we assessed the functional outcomes in sham animals ($n = 16$), vehicle-treated HI animals ($n = 21$), and AG490 pre-treated HI animals ($n = 15$). Short-term neurobehavioral tests included the evaluation of geotaxis reflex, cliff avoidance reflex, and grip tests. These were performed on 1, 3, and 7 days after HI. Compared with sham pups, the neurobehavioral functioning of pups in the vehicle-treated HI group was significantly impaired on all measured days after HI (Fig. 4, $p < 0.05$). The AG490-treated HI group performed significantly better in the geotaxis test 7 days after HI (Fig. 4b) compared with the vehicle-treated HI group (2.33 ± 0.25 versus 8.74 ± 1.63 s, respectively; $p < 0.05$). Three and seven days after HI, cliff avoidance reflex

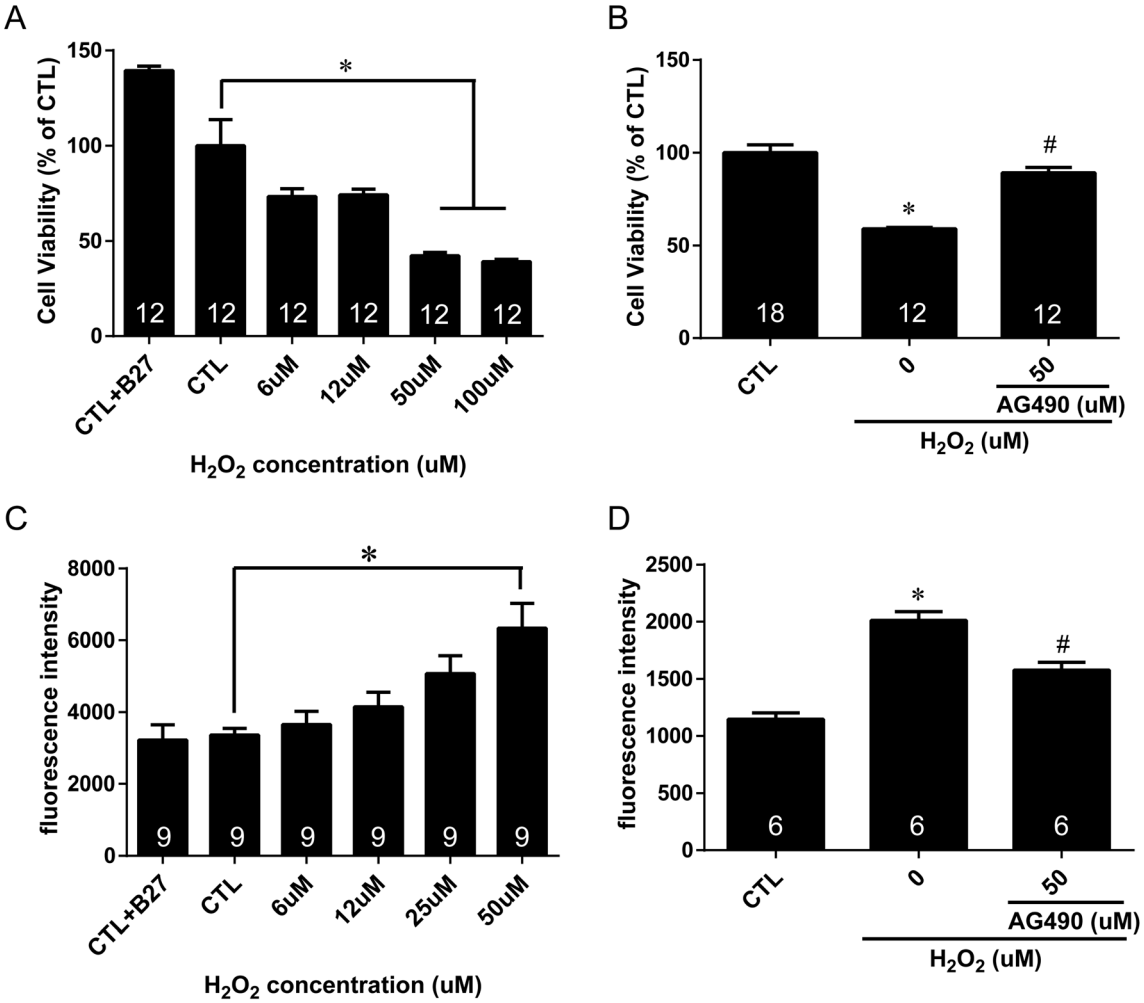

Fig. 2 Pre-treatment of cortical neurons with AG490 reduced cell death following H_2O_2-induced cell injury. **a** MTT assay to assess cell viability. Left, incubation with H_2O_2 (5% CO_2, 95% humidified air, 37 °C, 24 h) resulted in reduced survival of cortical neurons in a dose-dependent manner from 6 to 100 μM. Right, AG490 (50 μM) pre-treatment prior to H_2O_2 (50 μM) exposure reduced neuronal death. **b** PI staining to access cell death. Cortical neurons were similarly treated. Left, H_2O_2 incubation resulted in increased cell death in a dose-dependent manner. Right, 50 μM AG490 protected neurons from H_2O_2-induced injury (CTL, control; $^{*}p < 0.05$, versus CTL group; $^{\#}p < 0.05$, versus non-treated group)

performance was also significantly better in the AG490-treated HI group compared with the vehicle-treated HI group (2.58 ± 0.22 versus 4.36 ± 1.33 s, respectively, at 3 days after HI; 3.86 ± 0.85 versus 6.94 ± 1.15 s, respectively, at 7 days after HI; Fig. 4c, $p < 0.05$). Grip test performance was also significantly better on all measured days after HI in the AG490-treated HI group compared with the vehicle-treated HI group (Fig. 4d, $p < 0.05$). Therefore, we provide the first evidence showing that AG490 pre-treatment can improve short-term neurobehavioral outcomes after HI brain injury.

To assess whether AG490 pre-treatment can improve long-term functional recovery, we employed the passive avoidance test 4 weeks after HI brain injury and examined whether AG490 treatment attenuated HI-induced memory impairment. We found that mice in the AG490 treatment group showed significantly better memory function in comparison with the vehicle-treated HI mice. Specifically, there was a significantly longer latency to enter the dark room 24 h after foot shock (Fig. 5a; $p < 0.05$). Whole brains extracted 32 days after the HI procedure were used to assess morphology changes at this time point. Nissl staining was carried out to determine histological changes. As shown in Fig. 5b, there is a reduced ipsilateral liquefaction volume with AG490 treatment compared with vehicle-treated HI control (sham, 0, $n = 11$; vehicle, 49.65 ± 10.24%, $n = 8$; AG490, 24.22 ± 6.03%, $n = 10$). Our results show that AG490 pre-treatment can have lasting therapeutic implications by alleviating long-term neurobehavioral deficits following neonatal HI brain injury.

Activation of Reactive Astrocytes Is Suppressed with AG490 Pre-treatment To assess the effects of AG490 on apoptotic signaling and neuronal survival, we stained and analyzed the

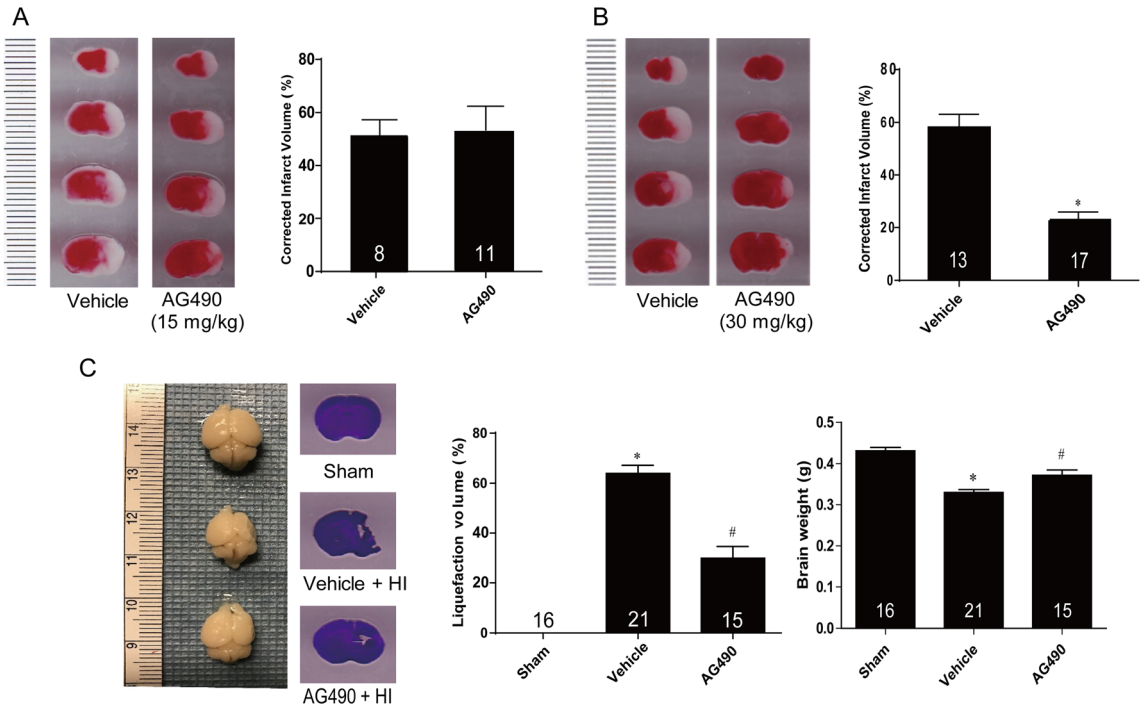

Fig. 3 In P7 mouse pups, pre-treatment with 30 mg/kg AG490 reduced infarct volume and improved overall brain morphology following HI brain injury. **a** At 15 mg/kg AG490 (chosen based on literature review ([38–41]), neuroprotective benefits were not observed. Representative TTC staining of brain slices with corresponding summary chart. **b** At 30 mg/kg, there was a reduction in brain infarct volume 24 h following HI brain injury. Left, representative TTC staining of brains from animals treated with either vehicle (5% DMSO + 5% Tween 80 in 0.9% saline) or AG490 (30 mg/kg) 20 min before the onset of injury (pre-treatment). Right, summary graph (*$p < 0.05$). **c** Overall brain morphology was preserved with AG490 (30 mg/kg) pre-treatment 7 days after HI injury. Left, representative whole brain images and Nissl staining to demonstrate the reduced liquefaction volume of the AG490-treated brain compared with vehicle control. Summary chart in the middle shows that ipsilateral liquefaction volume was significantly reduced with AG490 treatment compared with vehicle control. Summary chart in the right shows that brain weight was significantly higher with AG490 treatment compared with vehicle control (*$p < 0.05$, comparison of vehicle control versus sham group; $^{\#}p < 0.05$, comparison of AG490 treatment versus vehicle control)

penumbra area of brain slices in sham, vehicle-treated, and AG490-treated groups 7 days after HI injury. NeuN (a commonly used biomarker for neurons) is a neuronal nuclear antigen [23, 24, 42]. GFAP expression in astrocytes represents astroglial activation and reactive gliosis [23, 24, 42], which are hallmarks following neurodegenerative conditions. As shown in Fig. 6a, AG490 pre-treatment significantly reduced the loss of NeuN-positive cells when compared with the vehicle-treated HI group. For the vehicle treatment group, we also found upregulation of GFAP expression in astrocytes, which indicates reactive gliosis and astroglial activation. The expression of GFAP was significantly lower in the AG490 treatment group ($n = 3$; $p < 0.05$).

Mechanism Underlying the Neuroprotective Effects of AG490 May Be Partly Through Akt-Mediated Signaling Pathways During development, the p-Akt/t-Akt level is high at P7 in mice [43]. As shown in Fig. 6b, we found that HI injury significantly reduced Akt phosphorylation levels in the ipsilateral hemisphere ($n = 3$; $p < 0.05$). This indicates a reduction in the activity of the Akt, which has major implications in cellular survival [43, 44]. Because Akt is associated with pro-survival signaling pathway, we speculate that this down-regulation of Akt activity contributes to neuronal death following HI. Nevertheless, with AG490 pre-treatment, the levels of phosphorylated Akt are restored to normal levels. Nonetheless, it should be noted that there is mass neuronal death in the ipsilateral hemisphere 24 h after HI, and this can potentially reduce overall Akt expression. However, we mainly focused on the ratio of phosphorylated to total Akt, which would indicate its level of signaling activity. We speculate that Akt signaling can potentially be one underlying the mechanism of neuroprotection of AG490.

Post-treatment of AG490 Also Confers Neuroprotection In Vivo Instead of pre-treatment (i.e., injecting AG490 20 min prior to the onset of HI brain injury), we administrated AG490 immediately after ischemia induction to examine whether AG490 can also provide a neuroprotective effect in a post-treatment paradigm. Assessments of outcome were carried out with the same experimental approaches as for pre-treatment studies. TTC staining in Fig. 7a showed that AG490 administration (30 mg/kg, i.p.) immediately after ischemia induction also reduced brain damage in the neonatal

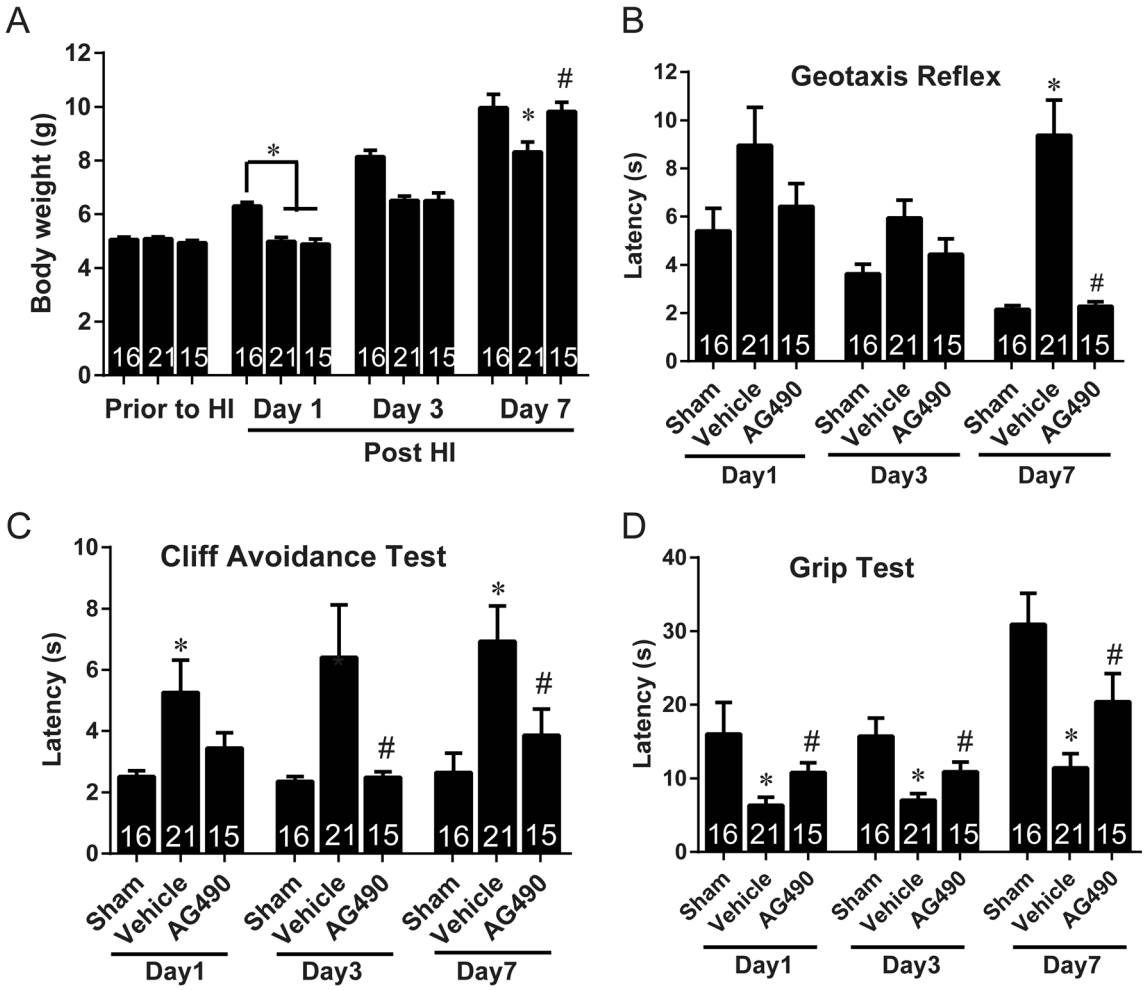

Fig. 4 AG490 pre-treatment improved general health and short-term neurobehavioral performance following HI brain injury. **a** Body weight, which is an indicator of recovery after HI, was significantly higher in sham and AG490 treatment groups than in vehicle control on the first and seventh days after HI (*$p < 0.05$, comparison of vehicle control versus sham group; #$p < 0.05$, comparison of AG490 treatment versus vehicle control). Columns from left to right represent: sham, vehicle control, and AG490 treatment (30 mg/kg), respectively, for each day measured. **b**–**d** Short-term neurobehavioral was evaluated with geotaxis reflex (**b**), cliff avoidance reflex (**c**), and grip test (**d**). Animals from all groups (i.e., sham, vehicle control, AG490 treatment) were measured on Days 1, 3, and 7 after HI (*$p < 0.05$ versus sham; #$p < 0.05$ versus vehicle control)

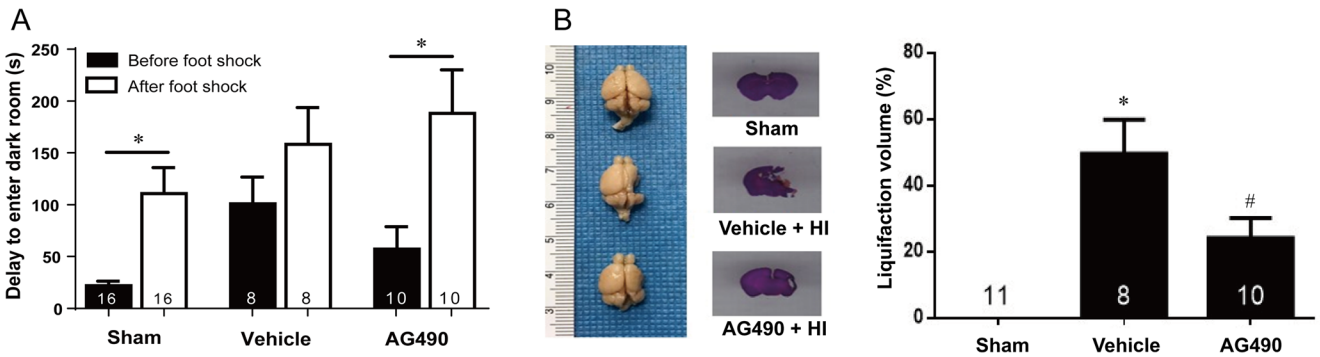

Fig. 5 Long-term behavioral performance 4 weeks after HI brain injury was also improved with pre-treatment of AG490. **a** In the passive avoidance test, AG490-treated (30 mg/kg) mice showed better memory function compared with vehicle-treated mice, as was evident from the significantly longer latency to enter the dark room 24 h after the foot shock conditioning (*$p < 0.05$). **b** Left, images of representative overall brain morphology and Nissl staining at 4 weeks after the HI time point. Brains pre-treated with AG490 show reduced liquefaction volume compared with vehicle control. Right, corresponding summary chart (*$p < 0.05$)

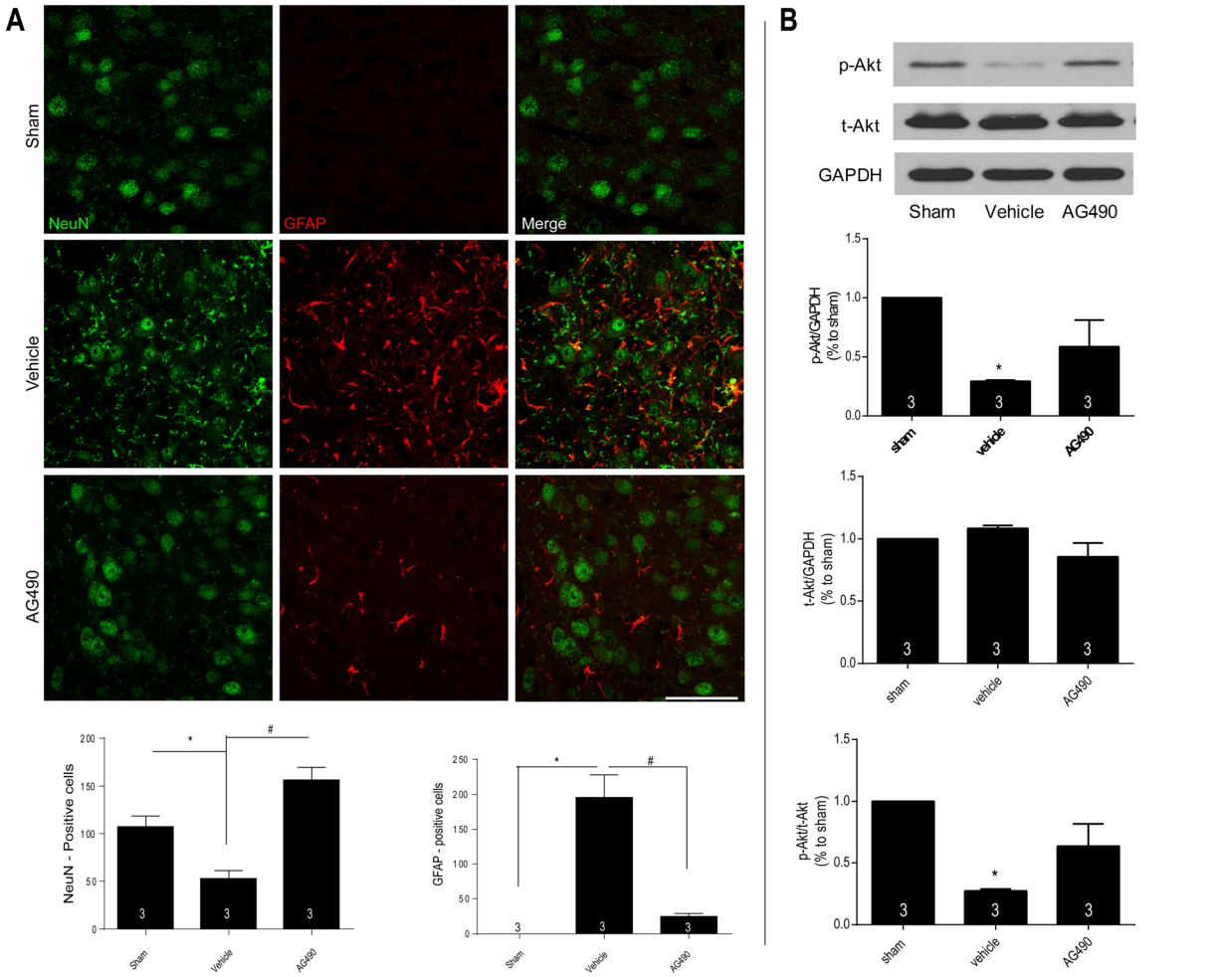

Fig. 6 AG490 pre-treatment restores neuronal cell numbers and reduces reactive astrocyte activation, potentially through Akt signaling as the underlying mechanism. **a** Left, representative confocal images of immunohistochemical staining (NeuN for neurons; GFAP for reactive astrocytes). AG490 (30 mg/kg) pre-treatment increased NeuN-positive cells (neurons) and decreased GFAP-positive cells (reactive astrocytes) compared with vehicle control. Right, summarizes NeuN- and GFAP-positive cells per × 40 field (*$p < 0.05$; #$p < 0.05$). **b** Left, representative Western blots of proteins extracted from the ipsilateral hemispheres of sham, vehicle control and AG490 pre-treatment groups 24 h after HI. Corresponding summary graphs show that Akt signaling was reduced with HI but was reversed with AG490 pre-treatment (*$p < 0.05$)

HI brain injury model (to 28.84 ± 3.61 from 50.51 ± 5.10%, $p < 0.05$).

In addition, whole brains were collected, fixed, and imaged 7 days after HI with the whole brain weights being measured. The AG490 post-treatment (30 mg/kg) group demonstrated significantly less brain damage in comparison with the vehicle treatment group (Fig. 7b, $n = 21$). Animals in the sham and AG490-treated HI groups had greater brain weights in comparison with the vehicle-treated HI group ($p < 0.05$). The liquefaction volume was also highest for vehicle-treated animals (sham, 0, $n = 5$; vehicle, 57.81 ± 2.43%, $n = 19$; AG490, 34.24 ± 3.91%, $n = 11$). Therefore, our results suggest that post-treatment of AG490 can also reduce brain damage following HI brain injury.

We also observed improvements in general recovery after HI, as well as in neurobehavioral performance with AG490 post-treatment. Body weight was measured and used to indicate general health of the pups. Similar to pre-treatment, pups were randomly assigned to different experimental groups with no initial significant differences (sham, 5.05 ± 0.08 g; vehicle-treated + HI, 5.08 ± 0.06 g; AG490-treated + HI, 4.93 ± 0.09 g). The body weights of each group were measured at four time points: before HI, 1, 3, and 7 days after HI (Fig. 8a). On Days 3 and 7 after HI, the mean body weight of pups in the vehicle-treated HI group was significantly lower than those in the sham and AG490-treated HI groups ($p < 0.05$). Therefore, post-treatment with AG490 promoted general recovery. As summarized in Fig. 8b–d, AG490 post-treatment also improved short-term neurobehavioral performances. Our salient findings provide evidence that AG490 can have therapeutic benefits as a post-treatment in response to hypoxia onset.

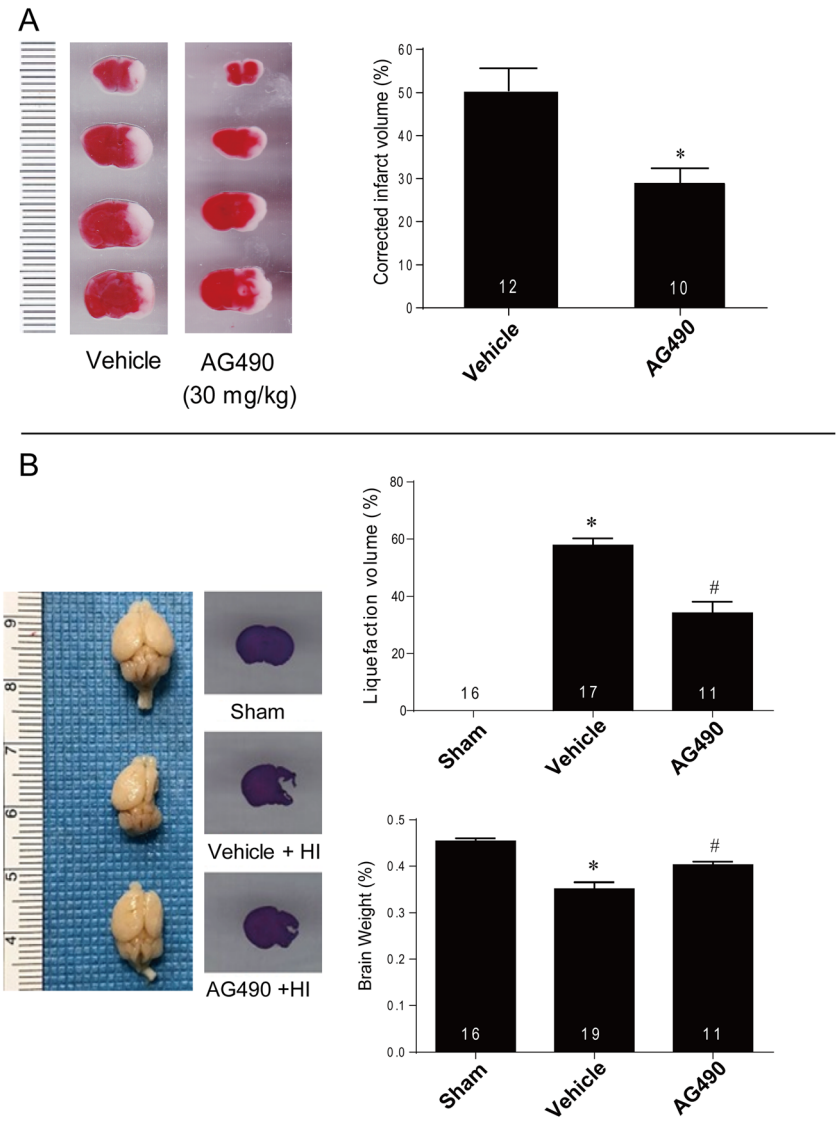

Fig. 7 Post-treatment with AG490 reduced brain infarct volume and brain damage following HI brain injury in vivo. **a** After 24 h. Representative TTC staining images and corresponding summary chart of correct brain infarction volume with or without AG490 (30 mg/kg, i.p.) post-treatment (i.e., immediately after ischemia; $^{*}p < 0.05$). **b** After 7 days. Left, representative whole brain images and Nissl staining. Right., corresponding summary charts of liquefaction volume and brain weight ($^{*}p < 0.05$ versus sham; $^{\#}p < 0.05$ versus vehicle control)

Discussion

Due to the lack of effective treatment for neonatal HI brain injury, surviving patients suffer from a drastic reduction in quality of life, and their families are burdened with lifetime healthcare costs. Given the global prevalence of this ailment and the poor long-term outcomes, novel neuroprotective treatments are urgently required. Neonatal HI brain injury has important differences compared with adult ischemic stroke [2]. For the infant brain, liquefactive disintegration can result from severe HI insults, but this is not observed following adult ischemic stroke [1]. Additionally, in neonates, blood vessels are more prone to rupture, and the blood-brain barrier is more severely compromised following HI insult [1, 2]. The autoregulation of the cerebrovasculature is drastically different for infants compared with adults [45]. Moreover, the expression and the actions of various signaling molecules, including caspase-3, are different in the developing brain [1]. Neonatal HI injury, but not adult ischemic stroke, can expand over time to other parts of the brain ([5]). Studies have shown that injuries within the initial hours following HI were subtle and isolated only in the putamen and the thalami, but then the injuries progressed over the next 3–4 days and diffused to other areas of the brain ([5]). Furthermore, the NMDA receptors are relatively overexpressed in the developing brain [46, 47]; in P6 rats, the NMDA receptor is expressed at 150–200% of the adult levels [48]. It has been speculated that the NMDA receptors are favored in the perinatal period to promote prolonged Ca^{2+} influx to elicit a level of excitation appropriate for development [49]. Increased level of glutamate has been found in the cerebrospinal fluid of infants who suffered from severe HI injury [50, 51]. The neonatal brain is more sensitive to seizures compared with the mature brain, suggesting a prominent role for neuronal hyperexcitability and excitotoxicity [52, 53]. In addition, neonatal brains are more vulnerable to H_2O_2 elevation, which has previously been

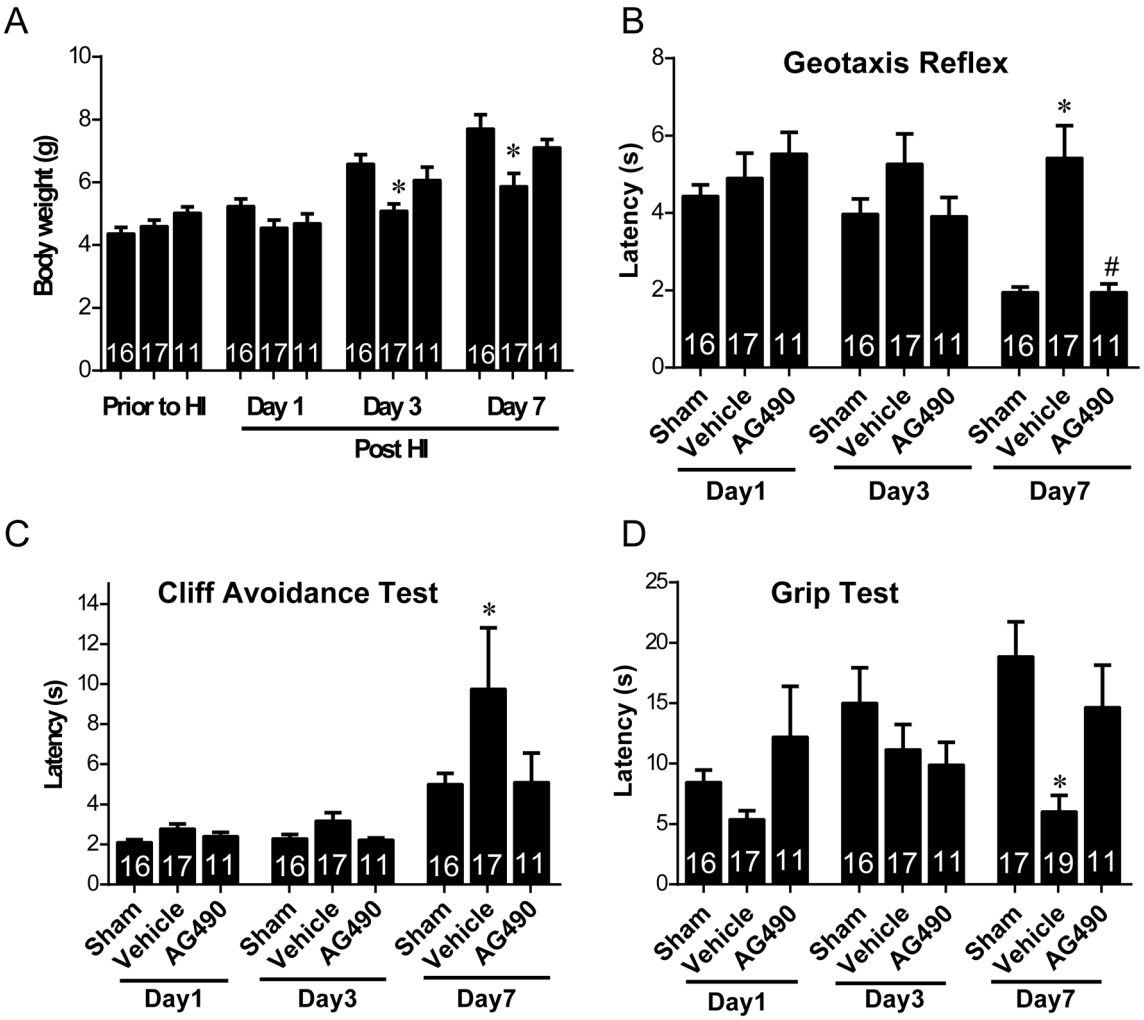

Fig. 8 AG490 (30 mg/kg) post-treatment improved general health and neurobehavioral performance after HI brain injury. **a** Body weight is an indication of general health. Weighing was done 1, 3, and 7 days after HI (*$p < 0.05$). Columns from left to right represent: sham, vehicle control, and AG490 treatment (30 mg/kg), respectively, for each day measured. **b**–**d** Neurobehavioral evaluation was accessed with geotaxis reflex (**b**), cliff avoidance reflex (**c**), and grip test (**d**) at 1, 3, and 7 days after HI (*$p < 0.05$ versus sham; #$p < 0.05$ versus vehicle control)

shown to be one of the characteristics following HI brain injury [54]. The accumulation of H_2O_2 coupled with low antioxidant activity results in sensitivity to oxidative stress.

Traditional glutamate-dependent mechanisms were traditionally considered to be the principal pathways involved in the ischemic cascade. Hence, glutamate receptors (i.e., NMDAR, AMPAR) were considered promising therapeutic targets [10]; specifically, inhibition of these receptors to reduce excitotoxicity. However, all clinical trials evaluating compounds that target glutamate receptors did not show beneficial neuroprotective outcomes [10]. And so, non-glutamate driven mechanisms have begun to gain attention. A major non-glutamate mechanism is mediated by TRPM2 channels, which have previously been implicated to be involved in numerous pathological processes including HI brain injury. The absence of TRPM2 activity by either siRNA silencing of TRPM2 in vitro [55] or knockout of TRPM2 in vivo [21] provided neuroprotective effects. Therefore, TRPM2 represents an important potential drug target. In the present study, we evaluated AG490, a compound previously shown to inhibit TRPM2 activity [22], in order to further elucidate the role of TRPM2 in neonatal HI brain injury. Ultimately, the goal is to evaluate whether pharmacological inhibition of TRPM2 can serve as a potential treatment for HI brain injury. Here, we employed both in vitro and in vivo models, via examining AG490 on the H_2O_2-induced neuronal cell death model, as well as in the mouse neonatal HI brain injury model.

Although classed as a JAK2 inhibitor [56], AG490 inhibits TRPM2 activity by scavenging hydroxyl radicals and not through Jak2-dependent mechanisms [22]. By using the H_2O_2-induced neuronal cell death model, we observed that AG490 increased neuronal survival. We then found in vivo that pre- or post-treatment with AG490 significantly reduced brain infarction volumes and preserved overall brain morphology 1, 7, and 32 days after HI. In addition, general health, short- and long-term functional recoveries after HI were

significantly improved with AG490 pre- or post-treatment. In addition, our evidence suggests that Akt signaling may be involved in the underlying mechanisms of this neuroprotective effect. That is, we demonstrated that HI injury significantly reduced Akt phosphorylation levels in the ipsilateral hemisphere, and that AG490 pre-treatment was able to restore this deficit. Nevertheless, the limitation in the present study is that AG490 also has effects on inhibiting JAK signaling (in addition to inhibiting H_2O_2-mediated activation of TRPM2). However, JAK inhibition is unlikely to contribute to the H_2O_2-meditated TRPM2 activation during the HI, as the previous study suggested that the inhibitory effects of AG490 on TRPM2 is independent of JAK2 inhibition [22]. However, it currently cannot be ruled out whether or not AG490-mediated JAK signaling can contribute to the overall neuroprotective effects seen in the present study. The molecular mechanism of neuroprotection mediated through the JAK2/STAT3 signaling pathway are controversial [57–62] and mainly focusing on adult ischemia stroke instead of neonatal HI brain injury [59, 60]. Since inhibition of TRPM2 has been implicated in neuroprotection against neonatal HI brain injury, we speculated that the effects of AG490 in reducing HI-induced brain damage are at least partially due to TRPM2 inhibition, independent of the JAK2 signaling pathways. Currently, there is no selective TRPM2 inhibitor available for in vivo study; when such a compound becomes available in the future, we will further test the effects of TRPM2 on HI brain injury.

The mechanism of neonatal HI brain injury remains ill-defined. Recent studies from our laboratory and others [21, 63] strongly suggest the involvement of the Akt/GSK-3β/caspase-3 signaling pathway. GSK-3, which consists of two isoforms GSK-3α and GSK-3β, was first identified as a regulatory protein for glycogen metabolism [64]. GSK-3 is involved in numerous cellular processes in the brain, including the Wnt-1/β-catenin and PI3K/Akt signaling pathways [64, 65]. Kinase activity of GSK-3 is inhibited through phosphorylation of GSK-3α or GSK-3β [64, 66]. Studies have shown that phosphorylation of Akt could inhibit GSK-3β kinase activity, which would consequently result in the downregulation of caspase-3-mediated apoptotic signaling [21]. This suggests that GSK-3β activity is linked to cell death. Our previous study [43] showed that TDZD-8, a specific GSK-3β antagonist, also confers neuroprotective effect against HI insult. Therefore, AG490's neuroprotective and therapeutic effects are potentially achieved through the reduction of Akt/GSK-3β/caspase-3 signaling, which ultimately favors the pro-survival signaling pathway. Further study is required to examine whether AG490 has any direct effects on GSK-3β/caspase-3. In summary, our present study demonstrates in vitro and in vivo the neuroprotective effects of AG490, with the broader implication that pharmacological inhibition of H_2O_2-mediated activation of TRPM2 can potentially be effective at providing neuroprotection for the treatment of neonatal HI brain injury.

Acknowledgments We also thank S Huang and W Chen for their technical assistance.

Funding This study is supported by grants to HSS from Natural Sciences and Engineering Research Council of Canada (NSERC) Discovery Grants (RGPIN-2016-04574) and to ZPF from the National Sciences and Engineering Research Council of Canada (RGPIN-2014-06471).

References

1. Millar LJ, Shi L, Hoerder-Suabedissen A, Molnár Z (2017) Neonatal hypoxia ischaemia: mechanisms, models, and therapeutic challenges. Front Cell Neurosci 78. https://doi.org/10.3389/fncel.2017.00078
2. Ferriero DM (2004) Neonatal Brain Injury. N Engl J Med 351: 1985–1995. https://doi.org/10.1056/NEJMra041996
3. Finer NN, Robertson CM, Richards RT, Pinnell LE, Peters KL (1981) Hypoxic-ischemic encephalopathy in term neonates: Perinatal factors and outcome. J Pediatr 98:112–117. https://doi.org/10.1016/S0022-3476(81)80555-0
4. Choi HA, Badjatia N, Mayer SA (2012) Hypothermia for acute brain injury—mechanisms and practical aspects. Nat Rev Neurol 8:214–222. https://doi.org/10.1038/nrneurol.2012.21
5. Fatemi A, Wilson MA, Michael VJ (2009) Hypoxic ischemic encephalopathy in the term infant. Clin Perinatol 36:835–858. https://doi.org/10.1016/j.clp.2009.07.011.Hypoxic
6. Gunn AJ, Battin M, Gluckman PD, Gunn TR, Bennet L (2005) Therapeutic hypothermia: from lab to NICU. J Perinat Med 33: 340–346. https://doi.org/10.1515/JPM.2005.061
7. Pauliah SS, Shankaran S, Wade A, Cady EB, Thayyil S (2013) Therapeutic hypothermia for neonatal encephalopathy in low- and middle-income countries: a systematic review and meta-analysis. PLoS One 8:e58834. https://doi.org/10.1371/journal.pone.0058834
8. Savman K, Brown KL (2010) Treating neonatal brain injury—promise and inherent research challenges. Recent Pat Inflamm Allergy Drug Discov 4:16–24
9. Arundine M, Tymianski M (2004) Molecular mechanisms of glutamate-dependent neurodegeneration in ischemia and traumatic brain injury. Cell Mol Life Sci 61:657–668. https://doi.org/10.1007/s00018-003-3319-x
10. Besancon E, Guo S, Lok J, Tymianski M, Lo EH (2008) Beyond NMDA and AMPA glutamate receptors: emerging mechanisms for ionic imbalance and cell death in stroke. Trends Pharmacol Sci 29: 268–275. https://doi.org/10.1016/j.tips.2008.02.003
11. Hetman M, Kharebava G (2006) Survival signaling pathways activated by NMDA receptors. Curr Top Med Chem 6:787–799
12. Gladstone DJ, Black SE, Hakim AM (2002) Toward wisdom from failure: lessons from neuroprotective stroke trials and new therapeutic directions. Stroke 33:2123–2136. https://doi.org/10.1161/01.STR.0000025518.34157.51
13. Aarts MM, Tymianski M (2005) TRPMs and neuronal cell death. Pflugers Arch - Eur J Physiol 451:243–249. https://doi.org/10.1007/s00424-005-1439-x
14. Eisfeld J, Lückhoff A (2007) TRPM2. Handb Exp Pharmacol 179: 237–252. https://doi.org/10.1007/978-3-540-34891-7_14
15. Jiang L-H, Yang W, Zou J, Beech DJ (2010) TRPM2 channel properties, functions and therapeutic potentials. Expert Opin Ther Targets 14:973–988. https://doi.org/10.1517/14728222.2010.510135
16. Gelderblom M, Melzer N, Schattling B, Göb E, Hicking G, Arunachalam P, Bittner S, Ufer F et al (2014) Transient receptor potential melastatin subfamily member 2 cation channel regulates

detrimental immune cell invasion in ischemic stroke. Stroke 45: 3395–3402. https://doi.org/10.1161/STROKEAHA.114.005836
17. Jang Y, Lee SH, Lee B, Jung S, Khalid A, Uchida K, Tominaga M, Jeon D et al (2015) TRPM2, a susceptibility gene for bipolar disorder, regulates glycogen synthase kinase-3 activity in the brain. J Neurosci 35:11811–11823. https://doi.org/10.1523/JNEUROSCI.5251-14.2015
18. Ostapchenko VG, Chen M, Guzman MS, Xie Y-F, Lavine N, Fan J, Beraldo FH, Martyn AC et al (2015) The transient receptor potential melastatin 2 (TRPM2) channel contributes to β-amyloid oligomer-related neurotoxicity and memory impairment. J Neurosci 35: 15157–15169. https://doi.org/10.1523/JNEUROSCI.4081-14.2015
19. Sumoza-Toledo A, Penner R (2011) TRPM2: a multifunctional ion channel for calcium signalling. J Physiol 589:1515–1525. https://doi.org/10.1113/jphysiol.2010.201855
20. Alim I, Teves L, Li R, Mori Y, Tymianski M (2013) Modulation of NMDAR subunit expression by TRPM2 channels regulates neuronal vulnerability to ischemic cell death. J Neurosci 33:17264–17277. https://doi.org/10.1523/JNEUROSCI.1729-13.2013
21. Huang S, Turlova E, Li F, Bao M-H, Szeto V, Wong R, Abussaud A, Wang H et al (2017) Transient receptor potential melastatin 2 channels (TRPM2) mediate neonatal hypoxic-ischemic brain injury in mice. Exp Neurol 296:32–40. https://doi.org/10.1016/j.expneurol.2017.06.023
22. Shimizu S, Yonezawa R, Hagiwara T, Yoshida T, Takahashi N, Hamano S, Negoro T, Toda T et al (2014) Inhibitory effects of AG490 on H_2O_2-induced TRPM2-mediated Ca^{2+}entry. Eur J Pharmacol 742:22–30. https://doi.org/10.1016/j.ejphar.2014.08.023
23. Chen WL, Turlova E, Sun CLF, Kim JS, Huang S, Zhong X, Guan YY, Wang GL et al (2015a) Xyloketal B suppresses glioblastoma cell proliferation and migration in vitro through inhibiting TRPM7-regulated PI3K/Akt and MEK/ERK signaling pathways. Mar Drugs 13:2505–2525. https://doi.org/10.3390/md13042505
24. Chen W, Xu B, Xiao A, Liu L, Fang X, Liu R, Turlova E, Barszczyk A et al (2015b) TRPM7 inhibitor carvacrol protects brain from neonatal hypoxic-ischemic injury. Mol Brain 8:11. https://doi.org/10.1186/s13041-015-0102-5
25. Sun H, Feng Z, Miki T, Seino S, French RJ, Feng Z, Miki T, Seino S et al (2006) Enhanced neuronal damage after ischemic insults in mice lacking Kir6.2-containing ATP-sensitive K+ channels. J Neurophysiol 95:2590–2601. https://doi.org/10.1152/jn.00970.2005
26. Wei W-L, Sun H-S, Olah ME, Sun X, Czerwinska E, Czerwinski W, Mori Y, Orser BA et al (2007) TRPM7 channels in hippocampal neurons detect levels of extracellular divalent cations. Proc Natl Acad Sci 104:16323–16328. https://doi.org/10.1073/pnas.0701149104
27. Rice JE 3rd, Vannucci RC, Brierley JB (1981) The influence of immaturity on hypoxic-ischemic brain damage in the rat. Ann Neurol 9:131–141. https://doi.org/10.1002/ana.410090206
28. Sun HS, Xu B, Chen W, Xiao A, Turlova E, Alibraham A, Barszczyk A, Bae CYJ et al (2015) Neuronal KATPchannels mediate hypoxic preconditioning and reduce subsequent neonatal hypoxic-ischemic brain injury. Exp Neurol 263:161–171. https://doi.org/10.1016/j.expneurol.2014.10.003
29. Xiao AJ, Chen W, Xu B, Liu R, Turlova E, Barszczyk A, Sun CL, Liu L et al (2015) Marine compound xyloketal B reduces neonatal hypoxic-ischemic brain injury. Mar Drugs 13:29–47. https://doi.org/10.3390/md13010029
30. Wong R, Abussaud A, Leung JW, Xu BF, Li FY, Huang S, Chen NH, Wang GL et al (2018) Blockade of the swelling-induced chloride current attenuates the mouse neonatal hypoxic-ischemic brain injury in vivo. Acta Pharmacol Sin 39:858–865. https://doi.org/10.1038/aps.2018.1
31. Xu B, Xiao A-J, Chen W, Turlova E, Liu R, Barszczyk A, Sun CLF, Liu L et al (2016) Neuroprotective effects of a PSD-95 inhibitor in neonatal hypoxic-ischemic brain injury. Mol Neurobiol 53:5962–5970. https://doi.org/10.1007/s12035-015-9488-4
32. Lubics A, Reglodi D, Tamás A, Kiss P, Szalai M, Szalontay L, Lengvári I (2005) Neurological reflexes and early motor behavior in rats subjected to neonatal hypoxic-ischemic injury. Behav Brain Res 157:157–165. https://doi.org/10.1016/j.bbr.2004.06.019
33. Castellano C, Pavone F (1988) Effects of ethanol on passive avoidance behavior in the mouse: involvement of GABAergic mechanisms. Pharmacol Biochem Behav 29:321–324. https://doi.org/10.1016/0091-3057(88)90163-3
34. Jarvik ME, Kopp R (1967) An improved one-trial passive avoidance learning situation. Psychol Rep 21:221–224. https://doi.org/10.2466/pr0.1967.21.1.221
35. Roberge S, Roussel J, Andersson DC, Meli AC, Vidal B, Blandel F, Lanner JT, Le Guennec JY et al (2014) TNF-alpha-mediated caspase-8 activation induces ROS production and TRPM2 activation in adult ventricular myocytes. Cardiovasc Res 103:90–99. https://doi.org/10.1093/cvr/cvu112
36. Allen Institute for Brain Science (2015) Allen mouse brain atlas. Allen Mouse Brain Atlas 445:168–176. https://doi.org/10.1038/nature05453
37. Workman AD, Charvet CJ, Clancy B, Darlington RB, Finlay BL (2013) Modeling transformations of neurodevelopmental sequences across mammalian species. J Neurosci 33:7368–7383. https://doi.org/10.1523/JNEUROSCI.5746-12.2013
38. Chai HT, Yip HK, Sun CK, Hsu SY, Leu S (2016) AG490 suppresses EPO-mediated activation of JAK2-STAT but enhances blood flow recovery in rats with critical limb ischemia. J Inflamm (United Kingdom) 13:18. https://doi.org/10.1186/s12950-016-0126-3
39. Davoodi-Semiromi A, Hassanzadeh A, Wasserfall CH, Droney A, Atkinson M (2012) Tyrphostin AG490 agent modestly but significantly prevents onset of type 1 in NOD mouse; implication of immunologic and metabolic effects of a Jak-stat pathway inhibitor. J Clin Immunol 32:1038–1047. https://doi.org/10.1007/s10875-012-9707-y
40. Higuchi T, Shiraishi T, Shirakusa T, Hirayama S, Shibaguchi H, Kuroki M, Hiratuka M, Yamamoto S et al (2005) Prevention of acute lung allograft rejection in rat by the Janus kinase 3 inhibitor, tyrphostin AG490. J Heart Lung Transplant 24:1557–1564. https://doi.org/10.1016/j.healun.2004.11.017
41. Toda T, Yamamoto S, Yonezawa R, Mori Y, Shimizu S (2016) Inhibitory effects of tyrphostin AG-related compounds on oxidative stress-sensitive transient receptor potential channel activation. Eur J Pharmacol 786:19–28. https://doi.org/10.1016/j.ejphar.2016.05.033
42. Turlova E, Bae CYJ, Deurloo M, Chen W, Barszczyk A, Horgen FD, Fleig A, Feng ZP et al (2016) TRPM7 regulates axonal outgrowth and maturation of primary hippocampal neurons. Mol Neurobiol 53:595–610. https://doi.org/10.1007/s12035-014-9032-y
43. Wang H, Huang S, Yan K, Fang X, Abussaud A, Martinez A, Sun HS, Feng ZP (2016) Tideglusib, a chemical inhibitor of GSK3β, attenuates hypoxic-ischemic brain injury in neonatal mice. Biochim Biophys Acta-Gen Subj 1860:2076–2085. https://doi.org/10.1016/j.bbagen.2016.06.027
44. Zhou H, Li XM, Meinkoth J, Pittman RN (2000) Akt regulates cell survival and apoptosis at a postmitochondrial level. J Cell Biol 151: 483–494. https://doi.org/10.1083/jcb.151.3.483
45. Volpe JJ (2012) Neonatal encephalopathy: An inadequate term for hypoxic-ischemic encephalopathy. Ann Neurol 72:156–166. https://doi.org/10.1002/ana.23647
46. McDonald JW, Roeser NF, Silverstein FS, Johnston MV (1989) Quantitative assessment of neuroprotection against NMDA-

induced brain injury. Exp Neurol 106:289–296. https://doi.org/10.1016/0014-4886(89)90162-3

47. Represa A, Tremblay E, Ben-Ari Y (1989) Transient increase of NMDA-binding sites in human hippocampus during development. Neurosci Lett 99:61–66. https://doi.org/10.1016/0304-394(89)90265-6
48. Tremblay E, Roisin MP, Represa A, Charriaut-Marlangue C, Ben-Ari Y (1988) Transient increased density of NMDA binding sites in the developing rat hippocampus. Brain Res 461:393–396. https://doi.org/10.1016/0006-8993(88)90275-2
49. Danysz W, Parsons CG (1998) Glycine and N-methyl-D-aspartate receptors: physiological significance and possible therapeutic applications. Pharmacol Rev 50:597–664
50. Hagberg H, Andersson P, Kjellmer I, Thiringer K, Thordstein M (1987) Extracellular overflow of glutamate, aspartate, GABA and taurine in the cortex and basal ganglia of fetal lambs during hypoxia-ischemia. Neurosci Lett 78:311–317. https://doi.org/10.1016/0304-3940(87)90379-X
51. Riikonen RS, Kero PO, Simell OG (1992) Excitatory amino acids in cerebrospinal fluid in neonatal asphysia. Pediatr Neurol 8:37–40. https://doi.org/10.1016/0887-8994(92)90050-9
52. Holmes GL (1991) The long-term effects of seizures on the developing brain: clinical and laboratory issues. Brain Dev 13:393–409. https://doi.org/10.1016/S0387-7604(12)80037-4
53. Holmes GL, Ben-Ari Y, Zipursky A (2001) The neurobiology and consequences of epilepsy in the developing brain. Pediatr Res 49:320–325. https://doi.org/10.1203/00006450-200103000-00004
54. Lafemina MJ, Sheldon RA, Ferriero DM (2006) Acute hypoxia-ischemia results in hydrogen peroxide accumulation in neonatal but not adult mouse brain. Pediatr Res 59:680–683. https://doi.org/10.1203/01.pdr.0000214891.35363.6a
55. Kaneko S, Kawakami S, Hara Y, Wakamori M, Itoh E, Minami T, Takada Y, Kume T et al (2006) A critical role of TRPM2 in neuronal cell death by hydrogen peroxide. J Pharmacol Sci 101:66–76
56. Seo IA, Lee HK, Shin YK, Lee SH, Seo S-Y, Park JW, Park HT (2009) Janus kinase 2 inhibitor AG490 inhibits the STAT3 signaling pathway by suppressing protein translation of gp130. Korean J Physiol Pharmacol 13:131–138. https://doi.org/10.4196/kjpp.2009.13.2.131
57. Digicaylioglu M, Lipton SA (2001) Erythropoietin-mediated neuroprotection involves cross-talk between Jak2 and NF-κB signalling cascades. Nature 412:641–647. https://doi.org/10.1038/35088074
58. Guo S, Li Z-Z, Gong J, Xiang M, Zhang P, Zhao G-N, Li M, Zheng A et al (2015) Oncostatin M confers neuroprotection against ischemic stroke. J Neurosci 35:12047–12062. https://doi.org/10.1523/JNEUROSCI.1800-15.2015
59. Satriotomo I, Bowen KK, Vemuganti R (2006) JAK2 and STAT3 activation contributes to neuronal damage following transient focal cerebral ischemia. J Neurochem 98:1353–1368. https://doi.org/10.1111/j.1471-4159.2006.04051.x
60. Wang X-L, Qiao C-M, Liu J-O, Li C-Y (2017) Inhibition of the SOCS1-JAK2-STAT3 signaling pathway confers neuroprotection in rats with ischemic stroke. Cell Physiol Biochem 44:85–98. https://doi.org/10.1159/000484585
61. Yoo S-J, Cho B, Lee D, Son G, Lee Y-B, Soo Han H, Kim E, Moon C et al (2017) The erythropoietin-derived peptide MK-X and erythropoietin have neuroprotective effects against ischemic brain damage. Cell Death Dis 8:e3003. https://doi.org/10.1038/cddis.2017.381
62. Zhu H, Zou L, Tian J, Du G, Gao Y (2013) SMND-309, a novel derivative of salvianolic acid B, protects rat brains ischemia and reperfusion injury by targeting the JAK2/STAT3 pathway. Eur J Pharmacol 714:23–31. https://doi.org/10.1016/j.ejphar.2013.05.043
63. Wu Y, Shang Y, Sun S, Liang H, Liu R (2007) Erythropoietin prevents PC12 cells from 1-methyl-4-phenylpyridinium ion-induced apoptosis via the Akt/GSK-3β/caspase-3 mediated signaling pathway. Apoptosis 12:1365–1375. https://doi.org/10.1007/s10495-007-0065-9
64. Beurel E, Grieco SF, Jope RS (2015) Glycogen synthase kinase-3 (GSK3): regulation, actions, and diseases. Pharmacol Ther 148:114–131. https://doi.org/10.1016/j.pharmthera.2014.11.016
65. Jope RS, Yuskaitis CJ, Beurel E (2007) Glycogen synthase kinase-3 (GSK3): inflammation, diseases, and therapeutics. Neurochem Res 32:577–595. https://doi.org/10.1007/s11064-006-9128-5
66. Shim SS, Stutzmann GE (2016) Inhibition of glycogen synthase kinase-3: an emerging target in the treatment of traumatic brain injury. J Neurotrauma 33:2065–2076. https://doi.org/10.1089/neu.2015.4177